Feedback Stabilization of a Permanent Magnet Levitation System

M. Reza Shariatmadari and Arash Komaee

Abstract—A magnetic levitation system consists of a magnet facing groundward to attract a magnetic object against gravity and levitate it at a distance from the face of magnet. Due to the unstable nature of this system, it must be stabilized by means of feedback control, which adjusts the magnetic force applied to the levitating object depending on its measured position and possibly velocity. Conventionally, electromagnets have been used for magnetic levitation, as they can be simply controlled via their terminal voltages. This paper, however, studies a levitation system relying on a permanent magnet and a linear servomotor to control the applied magnetic force by changing the distance between the magnet and the levitating object. For the proposed system, which is highly nonlinear, a stabilizing feedback control law is developed using feedback linearization and other control design tools. Then, the closed-loop stability is examined against system parameters such as the size of the levitating object, the viscosity of the medium it moves in, and certain characteristics of the magnet in use. The emphasis here is on understanding the impact of intrinsic servomotor limitations, particularly its f nite slew rate (cap on its maximum velocity), on the ability of feedback control to stabilize the closed-loop system. This particular limitation seems to be a major concern in utilizing permanent magnets for noncontact actuation and control.

I. INTRODUCTION

Magnetic levitation using electromagnets has been studied extensively in the literature (see [1] and references therein). In the simplest form, a magnetic levitation system consists of an electromagnet facing groundward to attract a magnetic object against gravity and maintain it at a f xed distance from the face of magnet. This goal cannot be achieved by simply applying some constant voltage to the electromagnet, since the equilibrium created by such constant voltage is inherently unstable. Instead, the voltage must be dynamically controlled by a stabilizing feedback loop including direct measurement of the instantaneous position of the magnetic object.

This paper considers a novel magnetic levitation system by replacing the electromagnet with the apparatus of Fig. 1 that consists of an axially magnetized permanent magnet bar and a linear servomotor to move it back and forth inside a guiding cylinder. In this magnetic levitation system, schematically shown in Fig. 2, control over the magnetic force is gained by manipulating the distance between the permanent magnet and the levitating object. Then, a feedback controller applies stabilizing reference values to the servomotor in terms of the measured values of the position, and possibly, the velocity of this object.

This work was supported by the National Science Foundation under Grant ECCS-1941944.

The authors are with the School of Electrical, Computer, and Biomedical Engineering, Southern Illinois University, Carbondale, IL, 62901 USA email: akomaee@siu.edu.



Fig. 1. Magnetic manipulator with a linear servomotor and an axially magnetized permanent magnet bar: (a) schematic diagram; (b) a 3D printed prototype. The dynamical model used for the analysis of this paper has been constructed based on this prototype, and its parameters have been extracted from empirical data collected through experiments on the prototype model.

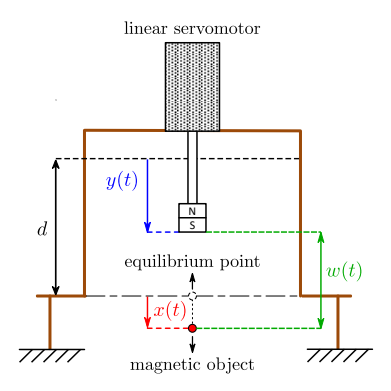


Fig. 2. Schematic diagram of a magnetic levitation system utilizing the permanent magnet manipulator in Fig. 1. This manipulator is positioned at the top of a rigid frame with its magnet faced toward ground. At a distance d from the face of magnet, the attractive magnetic force applied to a magnetic object cancels gravity. A feedback loop is established to stabilize the magnetic object at a point along the vertical axis.

The focus of this paper is on feedback control design and stability analysis of the magnetic levitation system of Fig. 2. The design procedure is complicated by the highly nonlinear dynamics of this system, originated in the nature of magnetic force and nonlinear limitations of the servomotor in use. To address these issues, a control design procedure is adopted in this paper based on two major control design tools, feedback linearization and linear quadratic regulator (LQR), enhanced by simulation-based numerical optimization techniques. The nonlinear control law designed via this procedure stabilizes the unstable equilibrium of the open-loop system, while maximizing the size of its region of attraction (ROA).

A major concern in stabilization of the magnetic levitation system of Fig. 2 is the intrinsic limitations of its servomotor. These limitations are twofold: f nite bandwidth, which is a linear phenomenon, and f nite slew rate (cap on the maximum velocity of the servomotor), which causes nonlinear behavior with severe consequences on closed-loop stability. The study of these limitations is a major goal of this paper, specifically to understand their impact on the ability of feedback control to stabilize permanent magnet levitation systems. This study

characterizes the ROA of the stabilized equilibrium point of these systems and investigates how the size of ROA depends on the servomotor limitations.

For a complete stability analysis, the dependence of ROA in other inf uential system parameters is examined, including the size of the levitating magnetic object, the viscosity of its surrounding medium, and the strength of magnet utilized by the magnetic levitation system. In particular, it is investigated how each of these parameters can boost or weaken the impact of a f nite slew rate of servomotor on the close-loop stability properties, specially, the size of ROA.

The numerical results of this study are generated by means of computer simulations, as discussed in Section IV. Yet, the dynamical model used for these simulations is empirically constructed by applying system identification procedures to the prototyped magnetic manipulator in Fig. 1(b). This model is presented in Section II and includes three components: an experimental characterization of magnetic force, a nonlinear state-space equation describing the servomotor dynamics and its limitations, and the equations of motion of the levitating magnetic object. We are currently working on a prototype model of the magnetic levitation system in Fig. 2 to verify the results of this paper experimentally.

This paper is an integral part of our broader efforts toward development of *noncontact magnetic manipulators* based on permanent magnets and mechanical actuators [2]–[9]. These manipulators present a transformative potential to develop new generations of minimally invasive medical procedures in which magnetized surgical tools or drug carriers navigate the natural pathways of the patient's body by precise control of external magnetic f elds [10]–[20]. These actuating magnetic f elds are generated and effectively controlled using spatial arrays of magnets arranged outside the patient's body. Such arrays of magnets are generically called noncontact magnetic manipulator, or simply, magnetic manipulator.

Magnetic manipulators have been conventionally designed as arrays of electromagnets f xed in space, simply controlled via their terminal voltages [21]–[26]. Yet, permanent magnets typically produce much stronger magnetic f elds compared to electromagnets of similar size, weight, and cost [27], offering a more attractive alternative for medical applications which often need strong magnetic forces at far distances of several decimeters away. To exploit this advantage, our research is dedicated to development of permanent magnet manipulators that control their magnetic f elds by proper movement of their magnets using mechanical actuators. For instance, massive electromagnets of a conventional magnetic manipulator can be replaced by compact units designed similar to Fig. 1.

Yet, replacement of electromagnets with a combination of permanent magnets and mechanical actuators raises certain concerns about the intrinsic limitations of these actuators, in particular their f nite slew rate and its impact on the stability of a permanent magnet manipulator. The magnetic levitation system in Fig. 2 is a simple permanent magnet manipulator with only a single magnet and a single direction of control, and therefore, can be conveniently used as a testbed for study of these concerns. The results of this paper for this simple

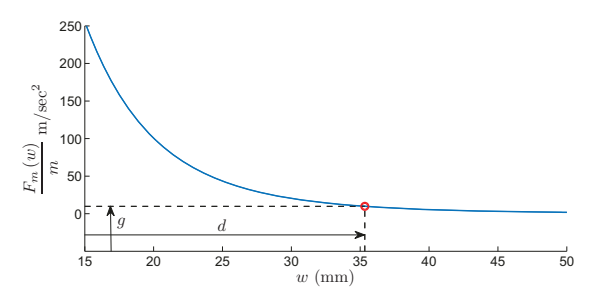


Fig. 3. Magnetic force per unit of mass (magnetic acceleration) versus distance from the face of magnet. At a distance d=35.33 mm from the face of magnet, the magnetic force cancels the gravity with the free-fall acceleration g=9.806 m/sec².

testbed provide insight into more complex designs including multiple magnets and multi-degree-of-freedom manipulation.

II. DYNAMICS OF MAGNETIC LEVITATION SYSTEM

This section develops a state-space model for the magnetic levitation system of Fig. 2. The overall model is presented in Section II-D and consists of an empirical model of magnetic force (Section II-A), a dynamical model of servomotor (Section II-B), and the equations of motion of a levitating magnetic object moving under the influence of a controlled magnetic force, gravity, and friction (Section II-C).

A. Empirical Model of Magnetic Force

In the context of this paper, a model of magnetic force is a scalar function $F_m\left(w\right)$ expressing the attractive force that the permanent magnet in Fig. 1 applies along its axis to a small magnetic object at a distance w from its face. This function is extracted from empirical data via the following procedure. Using a Senis MMS-1A-RS magnetic f eld scanner, the axial component $B\left(w\right)$ of the magnetic f eld is measured along the axis of the permanent magnet in a range of $15~\mathrm{mm}$ to $50~\mathrm{mm}$ from its face. Then, the magnetic force $F_m\left(w\right)$ is extracted from the recorded data using a known relationship between the magnetic f eld and magnetic force.

This relationship determines the magnetic force applied to a small magnetic object in terms of the spatial gradient of the magnetic feld at the location of the object [24]. For the axially symmetric magnet in Fig. 1, the magnetic force along its axis is given by

$$F_m(w) = \frac{m}{2\rho\mu_0} \cdot \frac{\chi}{1 + \chi/3} \cdot \frac{d}{dw} B^2(w), \qquad (1)$$

where m is the mass of the magnetic object, ρ is its density, χ is its magnetic susceptibility, and μ_0 denotes the permeability of free space. To derive a mathematically tractable expression for the magnetic force, a polynomial of order 5 was f tted to the empirical values of $1/B^2$ (w), and F_m (w) was estimated from (1). For the numerical values $\rho=7.8$ g/cm³, $\chi=10^3$, and $\mu_0=4\pi\times10^{-7}$ H/m, the estimated magnetic force per unit of mass (magnetic acceleration) is illustrated in Fig. 3.

B. Dynamical Model of Servomotor

The servomotor dynamics in the magnetic manipulator of Fig. 1 is governed by a second order nonlinear state-space equation, in which the nonlinear term represents the intrinsic

cap on the highest velocity that the servomotor and its fasten magnet can attain. In what follows, this equation is developed in two steps: f rst, the structure of equation is f xed, and then, its parameters are estimated from empirical data collected from experiments on the magnetic manipulator of Fig. 1(b). The goodness of f t is verif ed by comparing the step response of the derived model against its experimental counterpart.

As shown in Fig. 2, let y(t) denote the position of the rod end of the servomotor with respect to some reference. Also, let u(t) be the command input to the servomotor with respect to the same reference, so that for a constant input $u(t) = \bar{u}$, $y(\infty) = \bar{u}$ holds in the steady state. Denote the velocity of the servomotor rod by $v_y(t)$. Then, the servomotor dynamics is described in this paper by the set of state-space equations

$$\dot{y}(t) = v_y(t)$$

$$\dot{v}_y(t) = -\alpha v_y(t) + \operatorname{sat}\left(-\left(2\zeta\omega_n - \alpha\right)v_y(t) - \omega_n^2 y(t) + \omega_n^2 u(t); \alpha S\right).$$
 (2b)

Here, α , ζ , ω_n , and S are model parameters taking positive values, and the saturation function sat (\cdot) is defined as

$$\operatorname{sat}(\xi; L) = \min\{|\xi|, L\}\operatorname{sign}(\xi).$$

For any input $u\left(t\right)$ of a small enough amplitude, the sat $\left(\cdot\right)$ function in (2b) stays in its linear region, and as a result, the servomotor dynamics reduces to a second order linear system with the natural frequency ω_n and the damping ratio ζ . These system parameters were estimated empirically using system identification techniques. To that end, the servomotor was excited in its linear region by an input signal of small enough amplitude, and its output was recorded via its built-in position sensor. Then, the MATLAB system identification toolbox was used to estimate $\omega_n=39.8~\mathrm{sec}^{-1}$ and $\zeta=0.7$.

Two other parameters S and α can be estimated from the response of servomotor to a sufficiently large step input that maintains it in saturation for a long period of time. Such step response has been recorded experimentally and is illustrated in Fig. 4. The constant slop of the step response in this figure introduces a nonlinear phenomenon with crucial effect on the performance of permanent magnet manipulators. A quick investigation of the state-space equations (2) indicates that the constant slope of the step response in Fig. 4 represents the slew rate S in these equations. Thus, S=81.62 mm/sec was estimated from the empirical step response. Furthermore, the value of $1/\alpha$ is the time scale at which the step response reaches the constant-slope regime. To attain the closest match between experiment and model, $\alpha=67.0$ sec $^{-1}$ was chosen.

C. Equations of Motion

This section applies Newton's second law of motion to a magnetic object to determine its equations of motion under the magnetic levitation system of Fig. 2. This magnetic object is assumed to be a sphere of radius r and mass m that moves inside a fuid of viscosity η under an applied magnetic force and gravity.

Let $x\left(t\right)$ be the distance of this object from the equilibrium point shown in Fig. 2, and denote the velocity of the object by

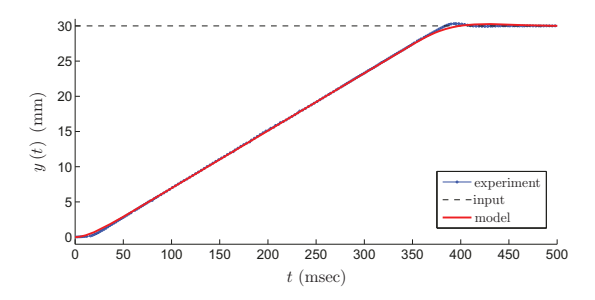


Fig. 4. Step response of the servomotor of Fig. 1 for a large 30 mm step, recorded from experiment (marked line), and determined from the developed model (solid line). The slew rate S of the servomotor has been estimated as the slope of the experimental step response. The numerical value of α has been calculated for the best match between experiment and model.

 $v_x\left(t\right)=\dot{x}\left(t\right)$. The magnetic object moves under three major forces: the Stokes drag $-6\pi r\eta v_x\left(t\right)$ [24], the gravitational force mg (g is the free-fall acceleration), and the magnetic force $F_m\left(w\left(t\right)\right)$ applied at a distance $w\left(t\right)=x\left(t\right)-y\left(t\right)+d$ from the face of magnet. Here, d>0 is a constant solving the algebraic equation $mg=F_m\left(d\right)$, as shown in Fig. 3 and represented geometrically in Fig. 2.

The dynamics of magnetic object is governed by Newton's second law of motion according to

$$m\dot{v}_x(t) = -6\pi r \eta v_x(t) + mg - F_m(x(t) - y(t) + d).$$

For simplicity of notation, this equation is rewritten as

$$\dot{v}_x(t) = -\sigma v_x(t) + a(x(t) - y(t)) \tag{3}$$

by defining the scalar function $a(\cdot)$ and the constant σ as

$$a(z) = g - \frac{F_m(z+d)}{m}, \qquad \sigma = \frac{9}{2} \cdot \frac{\eta}{\rho_m r^2}.$$
 (4)

D. Dynamical Model of the Magnetic Levitation System

By concatenating the trivial relationship $\dot{x}(t) = v_x(t)$, the equation of motion (3), and the servomotor dynamics (2), the overall dynamics of the magnetic levitation system in Fig. 2 is described by the nonlinear state-space equations

$$\dot{x}\left(t\right) = v_{x}\left(t\right) \tag{5a}$$

$$\dot{v}_x(t) = -\sigma v_x(t) + a(x(t) - y(t)) \tag{5b}$$

$$\dot{y}\left(t\right) = v_{y}\left(t\right) \tag{5c}$$

$$\dot{v}_{y}\left(t\right) = -\alpha v_{y}\left(t\right) + \operatorname{sat}\left(-\left(2\zeta\omega_{n} - \alpha\right)v_{y}\left(t\right) - \omega_{n}^{2}y\left(t\right) + \omega_{n}^{2}u\left(t\right); \alpha S\right). \tag{5d}$$

This nonlinear model is used in the remainder of this paper for both control design and computer simulations.

III. FEEDBACK STABILIZATION

This section is intended to design a state feedback law that stabilizes the unstable dynamics (5) around its equilibrium point (0,0,0,0) with the largest possible ROA. This control design problem is complicated by the nonlinear nature of the state-space equations (5) originating from two sources: the inherent nonlinear nature of magnetic force, and the f nite slew rate of the servomotor in use. Among these sources of nonlinearity, the contribution of magnetic force is completely compensated by feedback linearization techniques. However,

the impact of a finite slew rate cannot be fully compensated; it can be only minimized by a well-designed controller.

To develop such a controller, a three-step design procedure is adopted in this paper relying on two major control design tools: the LOR method and feedback linearization. At f rst in Section III-A, the LQR method is applied to develop a family of stabilizing linear feedback laws for a linear approximation of the state-space equations (5). Next in Section III-B, the nonliterary of magnetic force is compensated using feedback linearization. In the feedback linearization process, auxiliary state variables are chosen in such a manner that the exact feedback linearized system has the same structure of the approximate linearized model, and consequently, the family of linear controllers designed for the approximate model can be equally applied to the exact linearized system. Combining feedback linearization with a member of the family of linear controllers yields a nonlinear controller, which is optimized in Section III-C for the best family member maximizing the size of ROA associated with the stabilized equilibrium point.

A. Approximate Linearization

The nonlinear dynamics (5) is linearized at the origin by disregarding saturation in (5d) and approximating a(x-y) in (5b) with its f rst order Taylor expansion. Since a(0) = 0 in essence, this Taylor expansion is given by a'(0)(x-y), where $a'(\cdot)$ denotes the derivative of $a(\cdot)$. Then, the set of state-space equations (5) is approximated by

$$\dot{x}\left(t\right) = v_x\left(t\right) \tag{6a}$$

$$\dot{v}_x(t) = -\sigma v_x(t) + a'(0)\left(x(t) - y(t)\right) \tag{6b}$$

$$\dot{y}\left(t\right) = v_{y}\left(t\right) \tag{6c}$$

$$\dot{v}_{y}(t) = -2\zeta\omega_{n}v_{y}(t) - \omega_{n}^{2}y(t) + \omega_{n}^{2}u(t). \tag{6d}$$

This approximate linearized model is stabilized next using a linear state feedback of the form

$$u(t) = -(k_1 x(t) + k_2 v_x(t) + k_3 y(t) + k_4 v_y(t))$$
 (7)

in which the gain vector (k_1, k_2, k_3, k_4) is determined via the LQR method. In tuning the gain vector, two control goals are considered: f rst, to keep the closed-loop system stable, and second, to keep it unsaturated as much as possible. These goals are achieved by simultaneously keeping both x(t) and the argument of sat (\cdot) function in (5d) small, mathematically represented as minimizing the quadratic cost functional

$$J = \int_0^\infty \left(x^2(t) + \beta \left(-(2\zeta\omega_n - \alpha) v_y(t) - \omega_n^2 y(t) + \omega_n^2 u(t) \right)^2 \right) dt. \quad (8)$$

Here, $\beta > 0$ is a parameter to adjust the relative importance of two opposing control goals, and is used in Section III-C to optimize the overall control performance.

B. Feedback Linearization

The nonlinear effect of magnetic force on the dynamics of a magnetic levitation system can be compensated by means of feedback linearization. Specifically, by applying a suitable nonlinear state feedback to the magnetic levitation system, it demonstrates linear dynamics with respect to some suitably chosen state variables (if the servomotor is not in saturation).

In this paper, the feedback linearized system is described by a state vector $(x(t), v_x(t), \tilde{y}(t), \tilde{v}_y(t))$ in which the new state variables $\tilde{y}(t)$ and $\tilde{v}_y(t)$ are defined as

$$\tilde{y}(t) = x(t) - \frac{a(x(t) - y(t))}{a'(0)}$$
(9a)

$$\tilde{v}_{y}(t) = v_{x}(t) - \frac{a'(x(t) - y(t))(v_{x}(t) - v_{y}(t))}{a'(0)}.$$
 (9b)

Then, in terms of the control $\tilde{u}(t)$ of the feedback linearized system, the nonlinear state feedback

$$u = \frac{a'(0)}{a'(x-y)}\tilde{u} + y - \frac{a'(0)}{a'(x-y)}\left(x - \frac{a(x-y)}{a'(0)}\right) - \frac{1}{\omega_n^2}\left(\frac{a'(0)}{a'(x-y)} - 1\right)\left(a(x-y) - (\sigma - 2\zeta\omega_n)v_x\right) - \frac{1}{\omega_n^2} \cdot \frac{a''(x-y)}{a'(x-y)}\left(v_x - v_y\right)^2$$
(10)

is applied to the magnetic levitation system (5). Here, $a''(\cdot)$ is the second derivative of $a(\cdot)$, and for sake of simplicity, the dependence of variables on t is not explicitly shown. By applying the nonlinear state feedback (10) to the magnetic levitation system described by (5), its feedback linearized dynamics in the unsaturated region is governed by the exact linear model

$$\dot{x}(t) = v_x(t)$$

$$\dot{v}_x(t) = -\sigma v_x(t) + a'(0) \left(x(t) - \tilde{y}(t)\right)$$

$$\dot{\tilde{y}}(t) = \tilde{v}_y(t)$$

$$\dot{\tilde{v}}_y(t) = -2\zeta \omega_n \tilde{v}_y(t) - \omega_n^2 \tilde{y}(t) + \omega_n^2 \tilde{u}(t),$$

which is identical to the approximate linearized model (6).

As the feedback linearized dynamics is governed by the same approximate linear model (6), the linear control law (7) developed for the approximate model can be identically used for $\tilde{u}(t)$, that is

$$\tilde{u}(t) = -(k_1 x(t) + k_2 v_x(t) + k_3 \tilde{y}(t) + k_4 \tilde{v}_y(t)).$$

Replacing $\tilde{y}\left(t\right)$ and $\tilde{v}_{y}\left(t\right)$ in this control law by (9), and then substituting the resulting $\tilde{u}\left(t\right)$ to the right-hand side of (10) leads to a nonlinear state feedback law of the form

$$u(t) = \mu(x(t), v_x(t), y(t), v_y(t))$$
 (11)

for stabilization of the magnetic levitation system.

C. Performance Optimization

The nonlinear control law (11) is constructed in terms of the gain vector (k_1, k_2, k_3, k_4) which depends on the tuning parameter $\beta > 0$ in the cost functional (8). This parameter is chosen next to optimize the performance of feedback control when the nonlinear dynamics (5) of the magnetic levitation system is stabilized by the nonlinear state feedback (11). The particular goal is to maximize the size of ROA that contains the stabilized equilibrium point at the origin (0,0,0,0).

This ROA is a subset of \mathbb{R}^4 defined as the set of all initial states of the closed-loop system for which the state trajectory converges to (0,0,0,0) as $t\to\infty$. Certainly, construction of ROA in a 4D space is computationally expensive, and indeed not necessary in practice. To study the closed-loop stability, it is enough to focus on the initial states of the form $(x_0,0,0,0)$ and determine the range of x_0 for which the state trajectories converge to the origin. This range is a closed interval denoted by $\mathrm{ROA}' = [-x_L, x_H]$ and represents the intersection of the actual ROA with the hyperplanes $v_x = 0$, y = 0, and $v_y = 0$.

The optimization goal is to maximize the payoff function

$$P = \min \left\{ x_L, x_H \right\}$$

with respect to $\beta>0$. To ensure a fast enough closed-loop dynamics, a constraint is included to the problem, requiring a closed-loop settling time of at least $T_s=1$ sec. The settling time is defined here as the required time for the state vector to reach 2% of its initial magnitude. The optimization problem is solved numerically by repeated simulations of the dynamical system (5) under the state feedback (11).

IV. NUMERICAL RESULTS AND STABILITY ANALYSIS

The stabilization performance of the control law (11) was studied by computer simulations of the magnetic levitation system in Fig. 2 under closed-loop control. For this purpose, the nonlinear state feedback (11) was applied to the nonlinear state-space equations (5) and the equations were numerically solved for different initial states and parameter values using the ode45 function of MATLAB. The main objective of this study was to characterize the ROA associated with the equilibrium point at the origin (0,0,0,0).

By constructing ROA' under different values of the system parameters, the effect of these parameters on the closed-loop stability is investigated in Figs. 5 to 7. In Fig. 5, the stability interval ROA' is illustrated versus the slew rate S (maximum velocity of servomotor in Fig. 2) for a magnetic ball of 1 mm diameter levitated in environments of different viscosities. It is observed that ROA' expands as either the slew rate or the viscosity of environment increase. In particular, under the slew rate S=81.62 mm/sec of the real-world servomotor in Fig. 1(b), ROA' is [-1.3, 1.4] in vacuum, [-3.0, 4.7] in soybean oil, and [-6.5, 15.2] in corn syrup (in unit of mm). A more intuitive interpretation of these numbers is that if the magnetic object is pulled up by 3.0 mm or down by 4.7 mm from its equilibrium inside soybean oil, the feedback loop is able to bring it back to the equilibrium.

Fig. 6 shows how the dimension of magnetic object affects the size of ROA'. In this f gure, the stability interval ROA' is illustrated versus the radius r of a spherical magnetic object moving in olive oil. It is observed that a reduction in the size of this object improves the closed-loop stability by increasing the size of ROA'. This is not surprising, since (4) indicates that decreasing \sqrt{r} has the same impact on the Stokes drag (the f uid friction) as increasing the viscosity η . Heuristically speaking, an increased friction reduces the speed of magnetic object for the same magnetic force, and as a result, enables

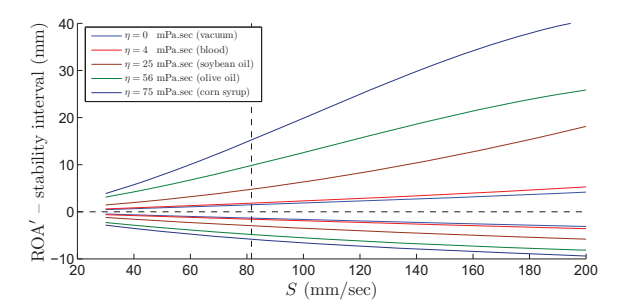


Fig. 5. Stability interval ROA' versus the slew rate S for a magnetic ball with 1 mm diameter moving in vacuum, blood, soybean oil, olive oil, and corn syrup. The vertical dashed line marks the slew rate $S=81.62 \, \mathrm{mm/sec}$ of the practical servomotor in Fig. 1(b).

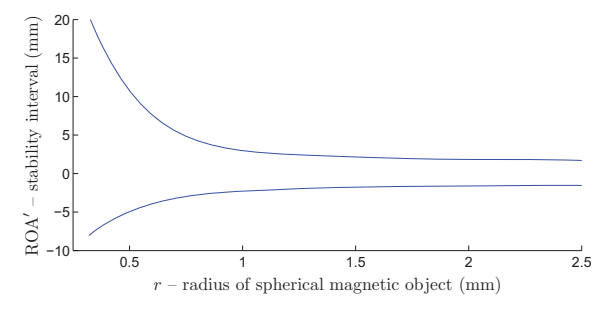


Fig. 6. Stability interval ROA' versus the radius r of a spherical magnetic object levitated in olive oil ($\eta=56$ mPa.sec) using the magnetic manipulator of Fig. 1(b) with the slew rate S=81.62 mm/sec.

the servomotor to more closely track the object, despite the limitation in its slew rate.

The ability of feedback control to stabilize the magnetic levitation system of Fig. 2 closely depends on the permanent magnet utilized in this system. Intuitively, a stronger magnet causes the magnetic object to move faster, which reduces the servomotor ability to closely track it. A closer look reveals that the closed-loop stability indeed depends on the slope of the magnetic force $F_m(w)$ at the equilibrium point, which in fact is proportional to the constant -a'(0) in the approximate linearized model (6).

To study this issue, the graph of Fig. 7 was created via the following procedure. First, a family of magnetic force curves was constructed by scaling the right-hand side of (1) by a factor of k ranging between 0.2 and 4. Each member of this family characterizes the magnetic force generated by a hypothetical permanent magnet which is k times stronger or weaker than the real-world magnet utilized in the magnetic manipulator of Fig. 1(b). For each hypothetical magnet, the distance d from the equilibrium point to the magnet face was obtained, the negative slope of the magnetic acceleration was computed at the equilibrium point according to

$$a'(0) = -\frac{1}{m} \cdot \frac{d}{dw} F_m(w) \Big|_{w=d},$$

and the stability interval ROA' was constructed. Then, ROA' was plotted in Fig. 7 versus a'(0) as k varies in [0.2, 4].

According to Fig. 7, the choice of permanent magnet has a signif cant impact in the closed-loop stability of the magnetic levitation system of Fig. 2. In selection or possibly design of a permanent magnet functionalized for levitation systems, the

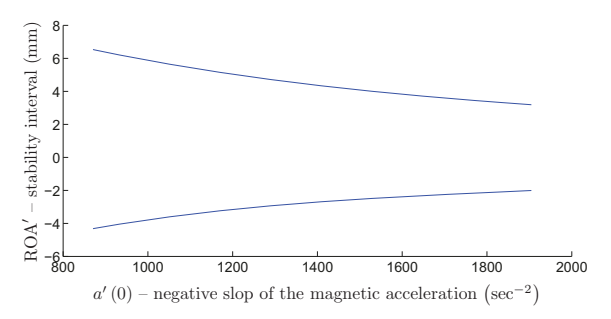


Fig. 7. Stability interval ROA' versus the negative slope a'(0) of the magnetic acceleration for a magnetic ball of 1 mm diameter levitated in soybean oil ($\eta=25$ mPa.sec) using the magnetic manipulator of Fig. 1(b) with the slew rate S=81.62 mm/sec.

guideline concluded from Fig. 7 is that a sound magnet must produce an axial magnetic force with slow spatial variations with respect to the distance from its face.

V. CONCLUSION

Feedback stabilization of a novel permanent-magnet-based levitation system was considered. Instead of the conventional approach which relies on electromagnets controlled via their terminal voltages, this system utilizes a permanent magnet controlled by a linear servomotor that can move it back and forth along a straight line. The magnet is faced groundward to attract a magnetic object against gravity and levitate it at an equilibrium point by feedback control of the servomotor. For the unstable, highly nonlinear dynamics of the proposed system, an experimental model was constructed and utilized then to develop a stabilizing nonlinear feedback law. Under this feedback law, the adverse impact of a finite slew rate of servomotor on the closed-loop stability was investigated. In addition, the closed-loop stability was examined against the size of the levitating object, the viscosity of medium it moves in, and characteristics of the permanent magnet in use.

REFERENCES

- [1] M. B. Khamesee, N. Kato, Y. Nomura, and T. Nakamura, "Design and control of a microrobotic system using magnetic levitation," *IEEE/ASME Trans. Mechatronics*, vol. 7, no. 1, pp. 1–14, 2002.
- [2] N. Riahi and A. Komaee, "Steering magnetic particles by feedback control of permanent magnet manipulators," in *Proc. of 2019 American Control Conference (ACC 2019)*, pp. 5432–5437, 2019.
- [3] N. Riahi, L. R. Tituaña, and A. Komaee, "Homotopy continuation for feedback linearization of noncontact magnetic manipulators," in *Proc.* of 2020 American Control Conference (ACC 2020), pp. 4295–4300, 2020.
- [4] N. Riahi and A. Komaee, "Noncontact steering of magnetic objects by optimal linear feedback control of permanent magnet manipulators," in Proc. of 2020 IEEE/ASME International Conference on Advanced Intelligent Mechatronics (AIM 2020), pp. 30–35, 2020.
- [5] L. R. Tituaña, "Implementation of a planar magnetic manipulator with rotatable permanent magnets," Master's thesis, Southern Illinois University, Carbondale, 2020.
- [6] M. Mohammadzadeh, M. R. Shariatmadari, N. Riahi, and A. Komaee, "Feedback decoupling of magnetically coupled actuators," in *Proceedings of the 2021 IEEE/ASME International Conference on Advanced Intelligent Mechatronics (AIM 2021)*, pp. 320–325, 2021.
- [7] T.-A. Sneed and A. Komaee, "Nonparametric reconstruction of vector f elds from noisy observations of their f ow curves," in *Proceedings of* the 2021 American Control Conference (ACC 2021), pp. 3959–3964, 2021.

- [8] N. Riahi, Design, Optimization, and Feedback Control of a Planar Noncontact Magnetic Manipulator With Rotatable Permanent Magnets. PhD thesis, Southern Illinois University, Carbondale, 2021.
- [9] M. R. Shariatmadari, "Feedback control and stability analysis of a permanent magnet levitation system," Master's thesis, Southern Illinois University, Carbondale, 2021.
- [10] M. Sendoh, K. Ishiyama, and K.-I. Arai, "Fabrication of magnetic actuator for use in a capsule endoscope," *IEEE Trans. Magn.*, vol. 39, no. 5, pp. 3232–3234, 2003.
- [11] G. Ciuti, P. Valdastri, A. Menciassi, and P. Dario, "Robotic magnetic steering and locomotion of capsule endoscope for diagnostic and surgical endoluminal procedures," *Robotica*, vol. 28, no. 2, pp. 199– 207, 2010.
- [12] M. Simi, P. Valdastri, C. Quaglia, A. Menciassi, and P. Dario, "Design, fabrication, and testing of a capsule with hybrid locomotion for gastrointestinal tract exploration," *IEEE/ASME Trans. Mechatronics*, vol. 15, no. 2, pp. 170–180, 2010.
- [13] A. Komaee and B. Shapiro, "Magnetic steering of a distributed ferrof uid spot towards a deep target with minimal spreading," in *Proc.* of 50th IEEE Conference on Decision and Control and European Control Conference, pp. 7950–7955, Dec. 2011.
- [14] S. Yim and M. Sitti, "Design and rolling locomotion of a magnetically actuated soft capsule endoscope," *IEEE Trans. Robot.*, vol. 28, no. 1, pp. 183–194, 2012.
- [15] A. Nacev, A. Komaee, A. Sarwar, R. Probst, S. H. Kim, M. Emmert-Buck, and B. Shapiro, "Towards control of magnetic fuids in patients: directing therapeutic nanoparticles to disease locations," *IEEE Control Syst. Mag.*, vol. 32, no. 3, pp. 32–74, 2012.
- [16] A. Komaee, R. Lee, A. Nacev, R. Probst, A. Sarwar, D. A. Depireux, K. J. Dormer, I. Rutel, and B. Shapiro, *Magnetic Nanoparticles: From Fabrication to Clinical Applications*, ch. Putting Therapeutic Nanoparticles Where They Need to Go by Magnet Systems Design and Control, pp. 419–448. CRC Press, 2012.
- [17] M. Beccani, C. Di Natali, L. J. Sliker, J. A. Schoen, M. E. Rentschler, and P. Valdastri, "Wireless tissue palpation for intraoperative detection of lumps in the soft tissue," *IEEE Trans. Biomed. Eng.*, vol. 61, no. 2, pp. 353–361, 2014.
- [18] V. Iacovacci, L. Ricotti, P. Dario, and A. Menciassi, "Design and development of a mechatronic system for noninvasive ref lling of implantable artificial pancreas," *IEEE/ASME Trans. Mechatronics*, vol. 20, no. 3, pp. 1160–1169, 2015.
- [19] L. Sliker, G. Ciuti, M. Rentschler, and A. Menciassi, "Magnetically driven medical devices: a review," *Expert Review of Medical Devices*, vol. 12, no. 6, pp. 737–752, 2015.
- [20] A. Komaee, "Feedback control for transportation of magnetic fuids with minimal dispersion: A frst step toward targeted magnetic drug delivery," *IEEE Trans. Control Syst. Technol.*, vol. 25, no. 1, pp. 129– 144, 2017.
- [21] E. G. Quate, K. G. Wika, M. A. Lawson, G. T. Gillies, R. C. Ritter, M. S. Grady, and M. A. Howard, "Goniometric motion controller for the superconducting coil in a magnetic Stereotaxis system," *IEEE Trans. Biomed. Eng.*, vol. 38, no. 9, pp. 899–905, 1991.
- [22] A. Komaee and B. Shapiro, "Steering a ferromagnetic particle by magnetic feedback control: Algorithm design and validation," in *Proc.* of 2010 American Control Conference (ACC 2010), pp. 6543–6548, 2010.
- [23] M. P. Kummer, J. J. Abbott, B. E. Kratochvil, R. Borer, A. Sengul, and B. J. Nelson, "OctoMag: An electromagnetic system for 5-DOF wireless micromanipulation," *IEEE Trans. Robot.*, vol. 26, no. 6, pp. 1006–1017, 2010.
- [24] R. Probst, J. Lin, A. Komaee, A. Nacev, Z. Cummins, and B. Shapiro, "Planar steering of a single ferrof uid drop by optimal minimum power dynamic feedback control of four electromagnets at a distance," J MAGN MAGN MATER, vol. 323, no. 7, pp. 885–896, 2011.
- [25] A. Komaee and B. Shapiro, "Steering a ferromagnetic particle by optimal magnetic feedback control," *IEEE Trans. Control Syst. Technol.*, vol. 20, no. 4, pp. 1011–1024, 2012.
- [26] S. Afshar, M. B. Khamesee, and A. Khajepour, "Optimal conf guration for electromagnets and coils in magnetic actuators," *IEEE Trans. Magn.*, vol. 49, no. 4, pp. 1372–1381, 2013.
- [27] O. Baun and P. Blümler, "Permanent magnet system to guide superparamagnetic particles," *J MAGN MAGN MATER*, vol. 439, pp. 294– 304, 2017.